

Research on defect quantification technique of Sparse array Total focusing method imaging based on Coherence factor weighting

Kang Da^{1,2}, Zhang Hong^{1,2}, ZHANG Yun-Miao¹, Wang Zi-Xin¹, MA Zhao-Guang¹,
Lin Shan-Shan¹, LI Jun-Jie¹

¹Beijing Power Machinery Research Institute, Beijing 100074, China; ²School of Mechanical Engineering and Automation, Beihang University, Beijing 100083, China

Abstract: Additive manufacturing technology is widely used in key components in the aerospace field due to its high manufacturing freedom and high precision. However, in the process of internal quality inspection of products, the signal attenuation caused by printing methods and materials brings certain challenges to the identification and quantification of defects. Total focusing method (TFM) is adopted to exploit FMC data and form an image where all pixels are focused in transmission and reception. The FMC–TFM approach is as highly accepted as the gold standard in ultrasonic imaging improve detection sensitivity and image resolution. However, the computational cost of TFM is substantial because it mainly operates in the time domain. In view of the above problems, this paper combines simulation and experimental verification, uses sparse matrix (SMC) set to carry out SMC-TFM imaging, and uses coherence factor (CF) weighted processing algorithm to enhance the SMC-TFM image and gets the SMC-TFM-CF image. On this basis, the quantitative characterization of defects of different sizes and orientations is realized, which can meet the needs of practical engineering.

Keywords: Sparse matrix capture; Total focusing method; Coherence factor; Defect quantification

1 Introduction

Additive manufacturing technology is widely used in the aerospace field^[1-3] with its advantages of high manufacturing freedom, high precision, saving time and raw materials, but in the process of additive manufacturing of parts due to heat, force and other influencing factors, cracks, pores, non-fusion and other defects will appear inside the parts. Phased array ultrasonic detection technology is widely used in the detection of additive products with the advantages such as adjustable sound beam^[4].

Phased array ultrasonic detection technology is developed on the basis of conventional ultrasonic detection technology, and it realizes the regulation and control of acoustic beams through signal delay and superposition. On this basis, Holmes^[5] et. al proposed a Total Focusing Method (TFM) based on full matrix data acquisition (FMC). FMC matrix is obtained by collecting signals from multiple directions through a unit composed of multiple pairs of elements, which contains more abundant defect information. Jobst M et al. applied Total focusing method^[6] imaging detection technology to weld quality detection, and conducted a comparative study on Total focusing method imaging images and fan scan images. The results show that TFM is the mainstream trend of weld detection in the future. Zhang^[7] J et al proposed multi-mode Total focusing method imaging on the basis of full focus of a single acoustic mode, and constructed a hybrid model based on scattering sparse matrix and sound line propagation. With the help of prior defect orientation and position information, it is helpful

to improve the detection performance of array. On the basis of the low efficiency of the existing FMC data integration image, Bannouf^[8] et al proposed a virtual point source total focusing method imaging based on the effective aperture, which can obtain the unknown of the excitation pulse and the activation element at the same time, and realize the optimization of the data set. P Y^[9] et al. proposed a new 2D sparse array design method based on genetic algorithm, including cross array and minimum redundancy array. Simulation and experimental results show that this method can effectively realize phased array ultrasonic detection. Yao Chen^[10] et al. applied the ring statistical factor weighting processing to the full focusing imaging in frequency domain, and improved the spatial resolution of the image by further utilizing the phase information.

In summary, on the basis of the above studies, this paper combined SMC-TFM imaging with Coherence factor weighting processing to achieve improved detection image quality, and verified the application of this method in the quantification of cracks of different sizes and orientations.

2 Imaging and crack quantification principle

2.1 Total focusing method imaging principle of sparse matrix data

The difference between Sparse Matrix Capture (SMC) Total focusing method imaging and conventional Total focusing method imaging mainly lies in the difference of data sets. Sparse matrix is based on certain criteria to determine the required excitation element number from the given number of matrix elements in advance. In this paper, genetic algorithm was used to determine the number of the required excitation elements in advance. The T_i element is excited successively to complete the data acquisition process of the corresponding R_i element. The data excitation and acceptance are shown in Figure 1, and the system sparse matrix is finally formed. The schematic diagram is shown in Figure 2.

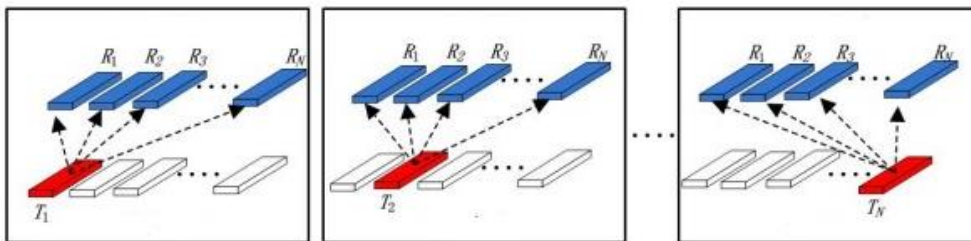


Figure 1 Schematic diagram of sparse array element transmitting and receiving

	R_1	R_3	R_{N-1}	R_N
T_1	A_{11}	A_{13}	A_{1i}	A_{1j}	$A_{1,N-1}$	$A_{1,N}$
T_3	A_{31}	A_{33}	A_{3i}	A_{3j}	$A_{3,N-1}$	$A_{3,N}$
⋮						
	A_{i1}	A_{i3}	A_{ii}	A_{ij}	$A_{i,N-1}$	$A_{i,N}$
⋮						
	A_{j1}	A_{j3}	A_{ji}	A_{jj}	$A_{j,N-1}$	$A_{j,N}$
⋮						
T_{N-1}	$A_{N-1,1}$	$A_{N-1,3}$	$A_{N-1,i}$	$A_{N-1,j}$	$A_{N-1,N-1}$	$A_{N-1,N}$
T_N	$A_{N,1}$	$A_{N,3}$	$A_{N,i}$	$A_{N,j}$	$A_{N,N-1}$	$A_{N,N}$

Figure 2 Schematic diagram of SMC data set

The principle of Total focusing method imaging is as follows: the target Region of Interest (ROI) required for Total focusing method imaging is discretized into several grid points with appropriate resolution, then each grid point can be regarded as a focal point; By controlling the signal time delay of each column A of SMC data set, the signal amplitude is superimposed on the focal point. After the superposition is completed, the gap between the amplitude of the defect and the non-defect position signal is further increased, so as to enhance the display of the defect signal and improve the image quality. The schematic diagram is shown in Figure 3.

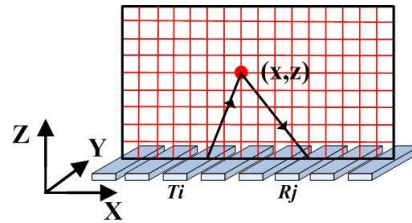


Figure 3 Schematic diagram of TFM principle

The sum of amplitudes superimposed by all N^2 A-scan signals on focal point (x, z) after delay is,

$$A_{TFM}(x, z) = \sum_{i=1}^N \sum_{j=1}^N A(Ti, Rj, t) \quad (1)$$

Where N is the number of elements and t is the delay time.

In the above formula, the propagation time t of Ti - Rj array combination through focal point (x, z) can be calculated by formula (2).

$$t = \frac{\sqrt{(x_{Ti} - x)^2 + z^2} + \sqrt{(x_{Rj} - x)^2 + z^2}}{c_l} \quad (2)$$

Where, x_{Ti} and x_{Rj} are respectively the horizontal coordinates of transmitting and receiving array elements, and c_l is the longitudinal wave sound velocity.

2.2 Quantitative principle of cracks

The defect length L and orientation are quantitatively characterized based on the coordinate position of the flaw space point of the crack. When there is an Angle between the crack and the propagation direction of sound wave, as shown in Figure 4, the echo at the lower tip of the open-cut crack on the bottom surface coincides with the echo at the bottom surface. The maximum value point of the echo at the top tip of the crack and the surface of the crack can be found, and a line segment can be made to determine the location of the lower tip by extending the line segment.

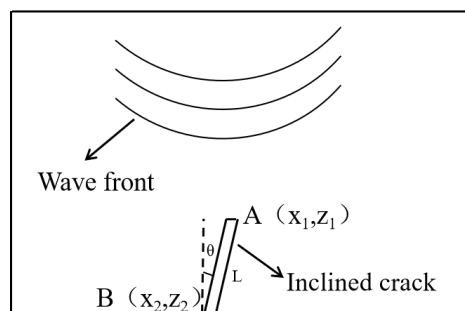


Figure 4 Quantitative principle of crack

Suppose that the coordinates of the top and bottom tips of the crack are A(x1, z1) and B(x2, z2), respectively. According to the above measurement method, the expressions of crack length L and the Angle between crack and acoustic wave propagation direction are respectively

$$L = \sqrt{(x_1 - x_2)^2 + (z_1 - z_2)^2} \quad (3)$$

$$\theta = \arctan\left(\frac{x_1 - x_2}{z_1 - z_2}\right) \quad (4)$$

2.3 Correlation Factor weighting Processing (Coherence Fcator)

Coherence Fcator (CF) is an adaptive weighted vector constructed based on the standard deviation of signal amplitude energy. Generally, CF is defined as the ratio of coherent energy to incoherent energy, and its expression is written as follows:

$$CF(x, z) = \frac{\left| \sum_{i=1}^N \sum_{j=1}^N A(T_i, R_j, t) \right|^2}{\sum_{i=1}^N \sum_{j=1}^N |A(T_i, R_j, t)|^2} \quad (5)$$

In the formula, the numerator term is the coherent energy term, expressed by the square of the sum of the focal point amplitudes in formula (1), and the denominator term is the coherent energy term, expressed by the square sum of the focal point amplitudes in formula (1). In this way, the formula (1) is weighted by the formula (5) to obtain the expression of the coherent factor full aggregation image:

$$A_{TFM-CF}(x, z) = A_{TFM}(x, z) \cdot CF(x, z) \quad (6)$$

3 Simulation modeling

CIVA software was used to establish a simulation model, the sound speed setting was consistent with the measured results, set to 5770m/s, and the sound speed fluctuation error was $\pm 10\%$, which was used to simulate the attenuation characteristics of additive manufacturing components; The center frequency of phased array probe was set to 10MHz, the number of array element was 64, Pitch0.6mm, Gap0.05mm; An opening slot on the bottom surface with a height of 2mm-10mm was set in the test block for simulating vertical cracks, as shown in Figure 5 (a); The length is 10mm, and the tilt Angle is 15° , 30° , 45° , 60° , 75° , which is used to simulate the tilt crack, as shown in Figure 5 (b).

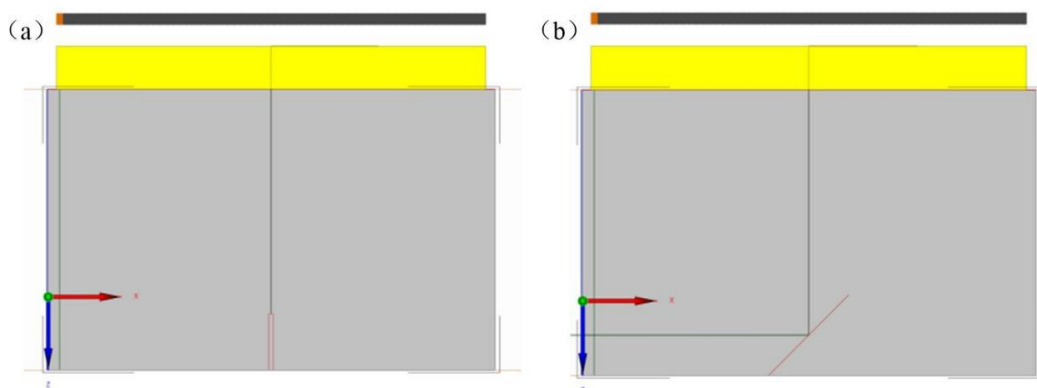


Figure 5 Simulation model of vertical and inclined crack: (a) vertical; (b) tilt

Sparse array data set was collected, and full focus imaging and coherence factor weighting were performed to obtain SMC-TFM-CF images, as shown in Figure 6 and Figure 7. Crack endpoint coordinate information was read according to defect quantification principle, and defect size information was calculated, as shown in Table 1 and Table 2.

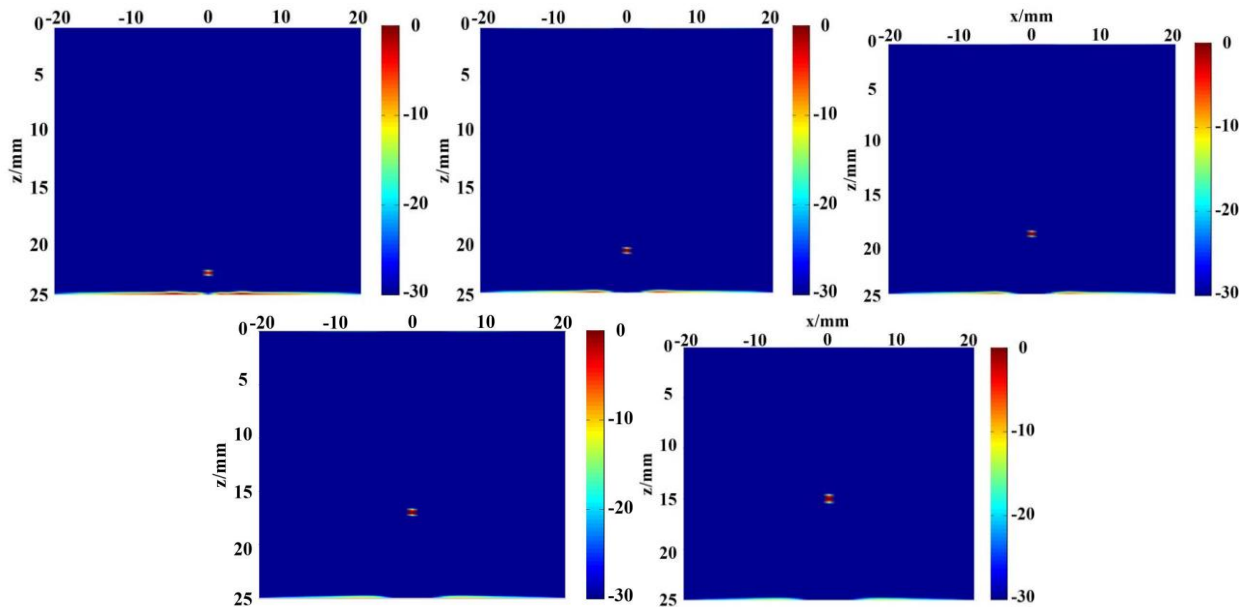


Figure 6 Simulation SMC-TFM-CF image of vertical crack

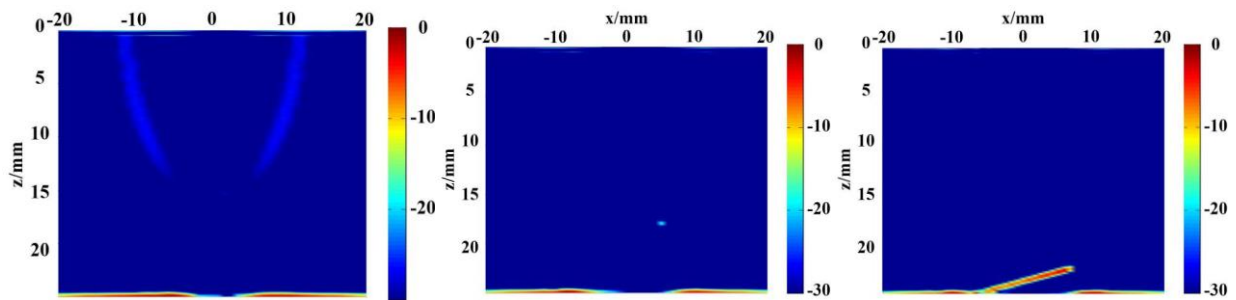


Figure 7 SMC-TFM-CF image of simulated tilt crack

Table 1 Measured values of simulated vertical cracks

Serial Number	Length (L) Default	SMC-TFM-CF measured values	Quantitative error
1	2mm	2.1 mm	0.1mm
2	3mm	3.1 mm	0.1 mm
3	4mm	4.1 mm	0.2 mm
4	5mm	5.1 mm	0.1 mm
5	6mm	6.0 mm	0
6	7mm	7.1 mm	0.1 mm
7	8mm	8.0 mm	0.2 mm
8	9mm	9.2 mm	0.2 mm
9	10mm	10.1 mm	0.1 mm

Table 2 Simulated oblique crack measured value

Serial Number	Length (L)/Tilt Angle () Default	SMC-TFM-CF measured values	Quantitative error
1	10mm/15°	9.7 mm / 13.8 °	-0.3 mm / 1.2 °
2	10mm/30°	10.3 mm / 31.1 °	0.3 mm / 1.1 °
3	10mm/45°	9.8 mm / 41.5 °	-0.2 mm / 1.5 °
4	10mm/60°	10.1 mm / 60.5 °	0.1 mm / 0.5 °
5	10mm/75°	10.6 mm / 74.2 °	0.6 mm / 0.8 °

4 experimental verification

The peak NDT phased array ultrasonic detector and Olympus phased array probe were used to carry out experimental data acquisition. The probe model is 10L-64-I1, as shown in Figure 8 (a). The same bottom open slot and inclined slot are prefabricated in the test block to simulate the crack type defects, as shown in Figure 8 (b). SMC matrix set was collected, full focus imaging and coherence factor weighting were performed in parallel, and SMC-TFM-CF images of vertical and inclined cracks as shown in FIG. 9 and 10 were obtained, and quantitative defect data were obtained statistically and calculated, as shown in Table 3 and Table 4.

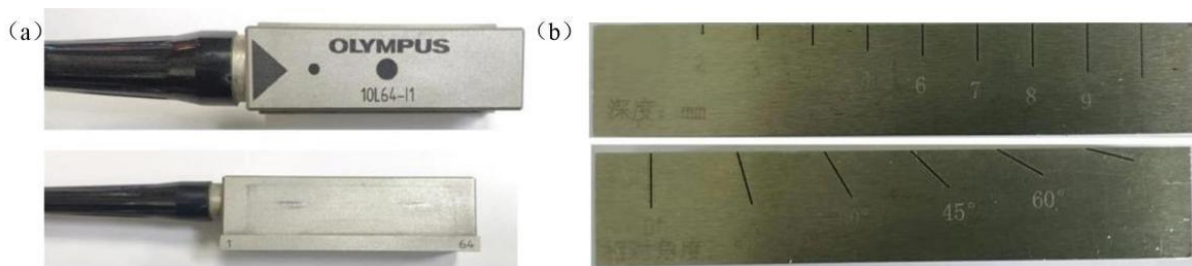


Figure 8 Actual pictures of the probe and crack test block for experiments: (a) probe; (b) test block

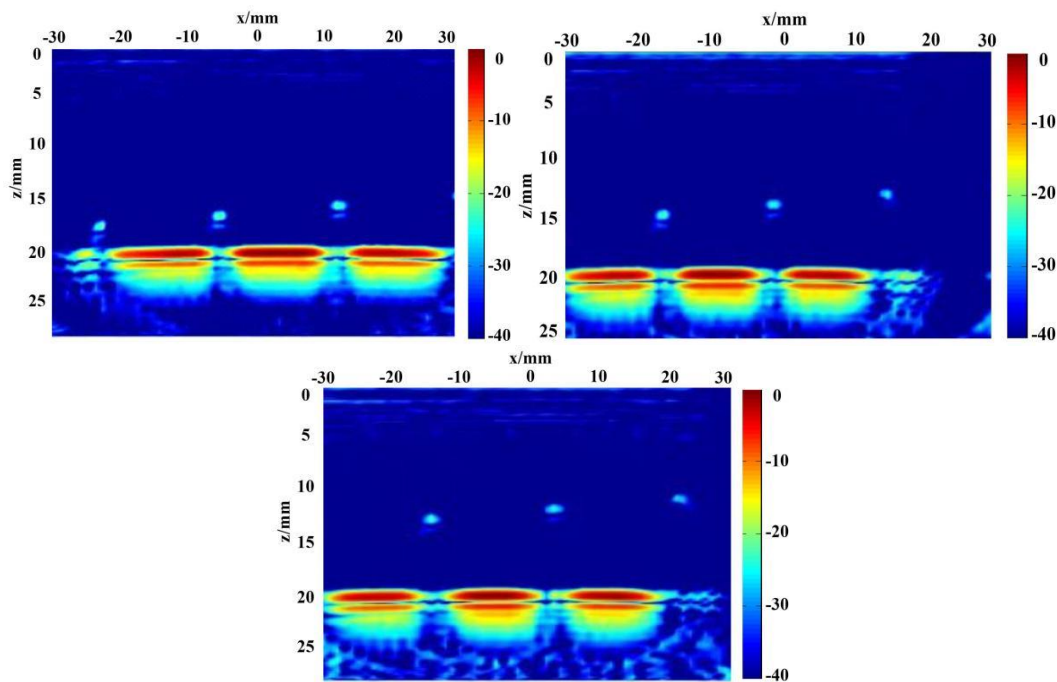


Figure 9 SMC-TFM-CF image of experimental vertical crack

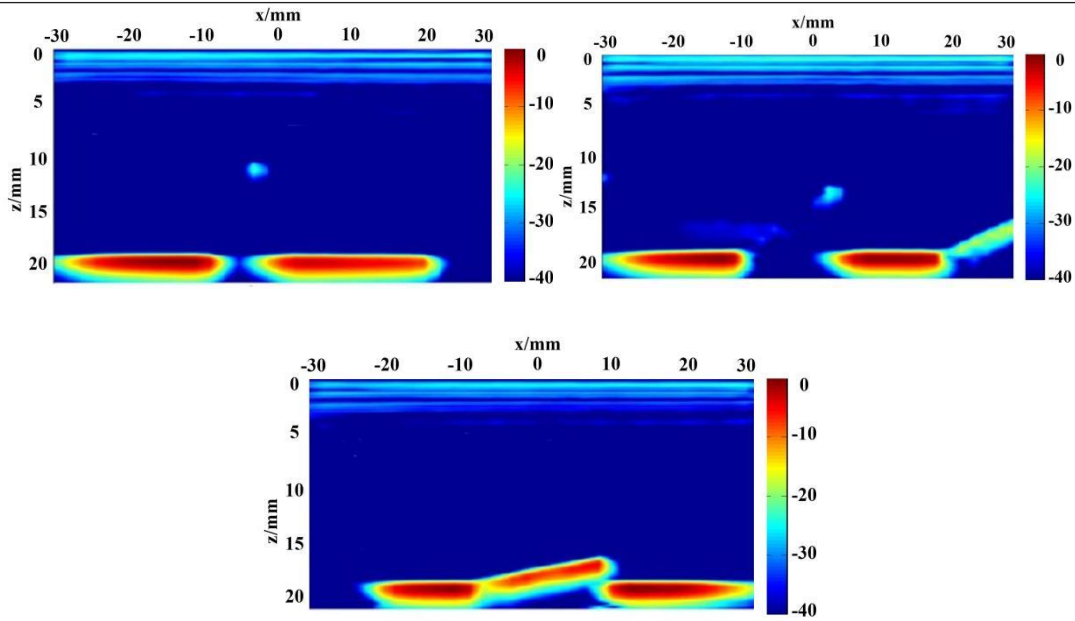


Figure 10 SMC-TFM-CF image of experimental inclined crack

Table 3 Measured values of experimental vertical cracks

Serial Number	Length (L) Preset	SMC-TFM-CF measured value	Quantitative error
1	2 mm	2.2 mm	0.2 mm
2	3 mm	3.2 mm	0.2 mm
3	4 mm	4.1 mm	0.1 mm
4	5 mm	5.1 mm	0.1 mm
5	6 mm	6.1 mm	0.1 mm
6	7 mm	7.1 mm	0.1 mm
7	8 mm	8.3 mm	0.3 mm
8	9 mm	9.2 mm	0.2 mm
9	10 mm	10.2 mm	0.2 mm

Table 4 Measured values of experimental tilt cracks

Serial Number	Length (L)/Tilt Angle () Default	SMC-TFM-CF measured value	Quantitative error
1	10 mm/15°	9.5 mm / 13.1 °	0.5 mm / 1.9 °
2	10 mm/30°	9.6 mm / 31.2 °	0.4 mm / 1.2 °
3	10 mm/45°	10.2 mm / 46.4 °	0.2 mm / 1.4 °
4	10 mm/60°	10.4 mm / 60.9 °	0.4 mm / 0.9 °
5	10 mm/75°	10.7 mm / 75.4 °	0.7 mm / 0.4 °

5 Discussion and Analysis

It can be seen from the simulation and experimental SMC-TFM-CF images that both can effectively identify vertical and inclined crack images and defect end point information. FIG. 11 shows the quantitative error comparison between the simulation and experimental vertical crack and inclined crack. It can be seen from the

figure that the maximum quantitative error of vertical crack length L is 0.3mm. The maximum quantitative error of inclined crack length L is 0.7mm, and the maximum quantitative error of inclined Angle q is 1.5° .

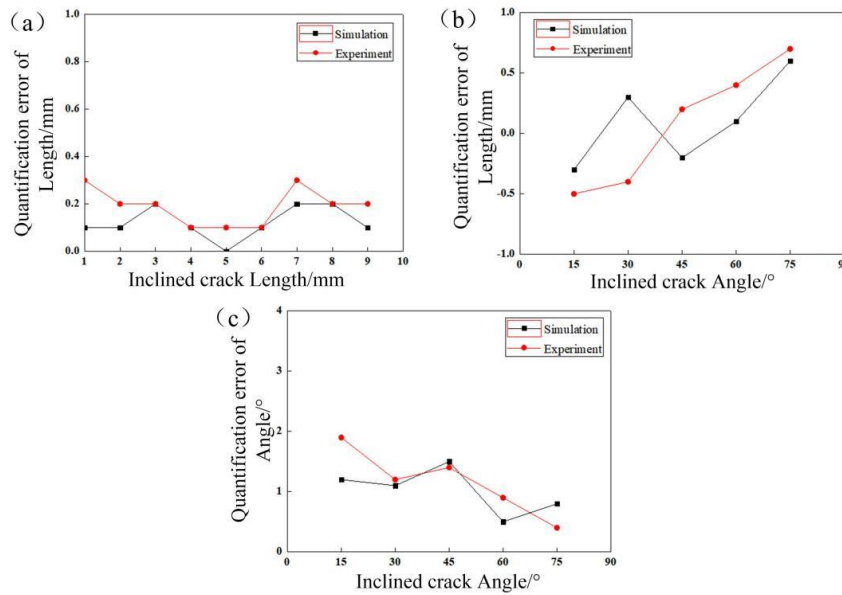


Figure 11 Statistical table of quantitative error of defects: (a) Quantitative error of vertical crack length; (b) Quantitative error of inclined crack length; (c) Quantitative error of inclined crack Angle

From the analysis of the above results, it can be seen that the variation trend of the experimental quantitative error is basically consistent with that of the simulation. The quantitative error of the vertical crack and the inclined crack is smaller than that of the length, and the maximum difference between them is 0.2mm. The maximum difference of quantitative error between experimental and simulation Angle of inclined crack is 0.7° . The quantitative error of vertical crack is larger than that of inclined crack. The reason for the quantitative error of length and inclined Angle above is that when quantifying vertical crack, the upper end of the defect can form an echo signal with stronger amplitude, which makes the location of the defect more accurate. The lower end of the defect is considered as the bottom wave of the test block, and the corresponding position information can be read more accurately. When quantifying inclined cracks, there are upper and lower endpoints and bottom waves. When the ultrasonic wave reaches the upper (or lower) tip of the defect, it is difficult to form an effective reflection surface, and the amplitude of the return wave will be weak, resulting in the echo signal received by the receiving array cannot form an effective echo waveform or the echo signal has little fluctuation. With the continuous propagation of the wave, the amplitude of the back wave is enhanced, the effective echo signal is formed, and the wave peak is the measured depth of the defect. However, the actual depth is about the starting position of the defect echo, resulting in an error of about half a wave width. In addition, the quantitative error of the experimental data is larger than that of the simulation in length and Angle. The main reason for this phenomenon is that the width of the echo signal of the experimental data is larger than that of the simulation due to the coupling, the wear of the phased array probe chip and the attenuation of materials during the experiment, which leads to certain errors in the statistical process of the upper and lower end points of the defect.

6 Conclusion

In this paper, the SMC-TFM is combined with the coherence factor weighting processing to realize the enhancement processing of the detection image of additive products. The SMC-TFM-CF method is used to

realize the effective identification and quantitative characterization of defects of different sizes and orientations, and the causes of quantitative errors are analyzed. The results show that this method is suitable for the internal quality detection and evaluation of key components in the field of aerospace, and can be applied in the subsequent practical projects.

Figure caption

Figure 1 Schematic diagram of sparse array element transmitting and receiving

Figure 2 Schematic diagram of SMC data set

Figure 3 Schematic diagram of TFM principle

Figure 4 Quantitative principle of crack

Figure 5 Simulation model of vertical and inclined crack: (a) vertical; (b) tilt

Figure 6 Simulation SMC-TFM-CF image of vertical crack

Figure 7 SMC-TFM-CF image of simulated tilt crack

Figure 8 Actual pictures of the probe and crack test block for experiments: (a) probe; (b) test block

Figure 9 SMC-TFM-CF image of experimental vertical crack

Figure 10 SMC-TFM-CF image of experimental inclined crack

Figure 11 Statistical table of quantitative error of defects: (a) Quantitative error of vertical crack length;(b) Quantitative error of inclined crack length; (c) Quantitative error of inclined crack Angle

References:

- [1] Conner, B.P., et al., Making sense of 3-D printing: Creating a map of additive manufacturing products and services. *Additive Manufacturing*, 2014. s 1 - 4: p. 64-76.
- [2] Huang, R., et al., Energy and Emissions Saving Potential of Additive Manufacturing: The Case of Lightweight Aircraft Components. *Journal of Cleaner Production*, 2015. 135: p. 1559-1570.
- [3] Yong, H. and S.R. Schmid, Additive Manufacturing for Health: State of the Art, Gaps and Needs, and Recommendations. *Journal of Manufacturing ence and Engineering*, 2018. 140(9): p. 094001.
- [4] Waller, J., et al., Summary of NDE of Additive Manufacturing Efforts in NASA. 2014.
- [5] Holmes, C., B.W. Brinkwater and P.D. Wilcox, Post-processing of the full matrix of ultrasonic transmit-receive array data for non-destructive evaluation. *NDT & E international: Independent nondestructive testing and evaluation*, 2005(8): p. 38.
- [6] Yan, L.I., Demonstration of Application of Total Focusing Method to Inspection of Steel Welds. *Nondestructive Testing Technology*, 2018.
- [7] Zhang, J., et al., Defect detection using ultrasonic arrays: The multi-mode total focusing method. *NDT & E International*, 2010. 43(2): p. 123-133.
- [8] Bannouf, S., et al., Data set reduction for ultrasonic TFM imaging using the effective aperture approach and virtual sources. *Journal of Physics Conference*, 2013. 457(1): p. 2007.
- [9] Ping, Y. Shi KeRen, A novel method to design 2D sparse array for ultrasonic phased array. *Applied Acoustics*, 2008. 27(2): p. 148-154.
- [10] Chen, Yao, Zhenghui tong, Qingru Kong, aoxiao Ma, Ming Chen, and Chao Lu. "Circular statistics vector for improving coherent plane wave compounding image in Fourier domain." *Ultrasonics* 128 (2023): 106856.